Nucleation-induced kinetic hindrance to the oxide formation during the initial oxidation of metals

Guangwen Zhou*
Department of Mechanical Engineering & Multidisciplinary Program in Materials Science and Engineering, State University of New York, Binghamton, New York 13902, USA
(Received 6 October 2009; published 27 May 2010)

A kinetic model is developed to elucidate the nucleation rate of oxide islands during the initial stages of oxidation of metals. Our theoretical analysis shows that the nucleation of oxide islands requires a critical oxygen pressure below which the nucleation rate is practically equal to zero and increases dramatically beyond it. The kinetic model shows that this critical oxygen pressure is many orders of magnitude larger than the equilibrium oxygen pressure predicted from the bulk thermodynamics. Comparison between the kinetic model and experimental data is made over a wide range of oxidation temperature.

DOI: 10.1103/PhysRevB.81.195440 PACS number(s): 81.65.Mq, 68.55.A−, 81.16.Pr

I. INTRODUCTION

The oxidation of metals plays a critical role in many important technological processes, such as corrosion, chemical catalysis, fuel reactions, and thin-film processing. The general reaction sequence of the oxidation on a clean metal surface is thought to proceed as oxygen surface chemisorption, oxide nucleation and growth, and then bulk oxide growth. Much is known about the oxygen surface chemisorption (adsorption of up to ~1 monolayer (ML) of oxygen), and particularly, the atomic structure of the chemisorbed phases on metal surfaces, as derived from surface-science studies under ultrahigh-vacuum (UHV) environments. In contrast, the growth of bulk oxides during both low- and high-temperature oxidation occurs usually under oxygen pressures much higher than those of the UHV conditions. Therefore, there is a wide gap between our present atomic-scale knowledge derived from conventional UHV experiments and the oxidation mechanisms obtained from the growth of bulk oxide thin films under high oxygen-pressure environments.

Despite the large pressure gap, a few experiments have in recent years significantly improved our atomic understanding of the initial oxidation of metal surfaces.[1–4] An intriguing phenomenon revealed from these studies is the existence of a kinetic hindrance to the oxide formation. Using *in situ* x-ray diffraction, Lundgren *et al.* monitored the oxidation processes of Pd(001) from oxygen surface chemisorption to the growth of PdO phase and found that the formation of PdO requires a surprising significantly larger oxygen pressure than that predicted by first-principles atomistic thermodynamics.[1] Similarly, the Cu-Cu_2O phase diagram determined by Eastman and co-workers using synchrotron x-ray scattering revealed a striking difference in behavior compared to the bulk phase diagram during the initial oxidation of Cu(001), with the Cu-Cu_2O phase boundary shifted several orders of magnitude upward in oxygen pressure for the formation of Cu_2O islands.[2] Their observation is also consistent with the study by Lyubinetsky *et al.*, who noted that the molecular beam epitaxy growth of single-phase Cu_2O nanoclusters could only be accomplished at many orders of magnitude larger oxygen pressure than the bulk Cu-Cu_2O phase boundary.[4]

Lahtonen *et al.*[3] reported more recently a study using combined *in situ* x-ray photoelectron spectroscopy and UHV scanning tunneling microscopy (STM) techniques to monitor the surface chemistry and the surface structure during the initial oxidation of a Cu(001) surface at 100 °C over a wide range of oxygen exposures and oxygen pressures (p_{O_2}). Figure 1 is derived from their work, in the low-pressure regime of $p_{O_2}=6.0\times10^{-7}$ Torr [Fig. 1(a)], the initial oxidation rate (in terms of the rate of oxygen uptake) is high until the oxygen coverage reaches 0.3 ML, which signals the onset of the $(2\sqrt{2}\times\sqrt{2})R45°$-O missing-row reconstruction induced by oxygen surface chemisorption, and then saturates at 0.5 ML corresponding to the formation of a nearly complete layer of the missing-row structure on the metal surface. This missing-row structure was found quite stable and highly inert toward further oxidation even after an increase in several orders of magnitude both in oxygen exposure and oxygen pressure. The oxygen uptake was observed to take place again on the same surface only after the oxygen pressure was further raised by five orders of magnitude, as shown in Fig. 1(b), where the oxygen pressure was at 2.8×10^{-2} Torr. This increase in oxygen uptake corresponds to the onset of the nucleation of Cu_2O-like three-dimensional (3D) islands on the reconstructed Cu(001) surface, as shown by the inset STM image in Fig. 1(b).[3]

The required significantly large oxygen pressure for the oxide formation is unexpected from the thermodynamics point of view. According to the well-known theoretical model by King and coworkers,[5–9] the transition from a chemisorbed oxygen layer to the initial appearance of an oxide phase is controlled thermodynamically, i.e., the oxide growth should set in immediately as soon as it is thermodynamically possible.[1] Lundgren *et al.* attributed the high p_{O_2} needed for the oxide formation to the oxygen-chemisorbed surface layer that creates a kinetic hindrance by impeding massive surface restructuring.[1] However, *in situ* STM images by Lahtonen *et al.* [as shown in the inset in Fig. 1(b)] show that the $(2\sqrt{2}\times\sqrt{2})R45°$-O missing-row structure remains quite stable during the nucleation of oxide islands under the high p_{O_2}, including the reconstructed surface regions adjacent to Cu_2O islands, suggesting that the oxide nucleation only involves very localized regions of the metal substrate

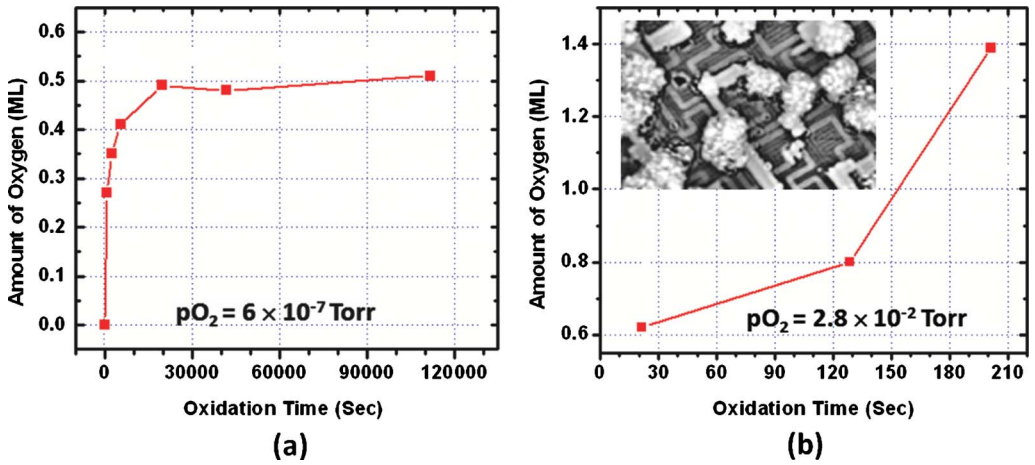

FIG. 1. (Color online) Surface oxidation kinetics on Cu(001) at 100 °C and two different oxygen pressures, (a) $p_{O_2}=6\times10^{-7}$ Torr; (b) $p_{O_2}=2.8\times10^{-2}$ Torr, the inset STM image shows nucleation of Cu_2O islands on the Cu surface under this oxygen partial pressure. The oxygen uptake saturates at 0.5 monolayer (ML) for the low P_{O_2} while taking place again on the same surface when the oxygen pressure is raised to 2.8×10^{-2} Torr, suggesting a critical p_{O_2} is needed in order to nucleate oxide islands on the metal surface. The data is derived from the Ref. 3 and the solid lines are shown to guide the eyes.

and such a process does not require massive restructuring of the metal surface. This is also consistent with the *in situ* x-ray results by Eastman *et al.*, which demonstrate that the intensity of the diffraction peak associated with the oxygen-chemisorbed surface layer remains unchanged with the gradual appearance of Cu_2O diffraction peaks due to the nucleation of Cu_2O islands during the oxidation of a Cu(001) surface.[2] So the question is what causes the kinetic hindrance to the oxide formation if the massive surface reconstructing is not the case. Correct answer to this question is not only very important for proper interpretation of experimental results but also crucial for manipulating early-stage oxidation processes for many practical applications such as high-pressure oxidation catalysis and controlled growth of oxide nanostructures. In the present work, we address this issue by modeling the kinetic factors of oxide nucleation processes, which reveals that this kinetic hindrance can be simply related to the oxide nucleation rate that is negligibly small until the oxygen pressure reaches a critical value at which the nucleation rate suddenly and dramatically increases.

II. KINETICS OF HETEROGENEOUS NUCLEATION OF OXIDE ISLANDS

The kinetic model to be developed is based on the assumption of heterogeneous nucleation of 3D oxide islands on a metal surface, as observed experimentally in many metal and alloy systems such as Cu,[2,3,10–14] Pd,[15,16] Ni,[15,17,18] Fe,[19] Cu-Au,[20,21] Cu-Ni,[22,23] and Co-Ni.[24] A general and simple picture of 3D nucleation of oxide islands during the oxidation of metals can be described as follows.[10,12,14,17,24–26] Oxygen-gas molecules impinge on the metal surface and dissociate. Dissociated O atoms diffuse over the metal surface and form a chemisorbed layer. Further coming oxygen may react with underlying substrate atoms to form oxide nuclei or be lost to reevaporation. The kinetics of oxide nucleation depends on the surface diffusivity of oxygen atoms as well as the nucleation barrier, which can be determined by the change in Gibbs free energy ΔG associated with the formation of an oxide embryo. Because the oxide nucleation requires reaction between oxygen atoms and the underlying substrate atoms, this causes oxide nuclei embedding into the metal substrate, as shown schematically in Fig. 2, where θ_1 and θ_2 are the contact angles of the double cap-shaped oxide island with the metal substrate, and σ_{NO}, σ_{NS}, and σ_{SO} are the interface energies for the interfaces between the nucleus and oxygen gas, nucleus and substrate, and substrate and oxygen gas, respectively. To catch these interfacial reaction effects, we introduce a recently developed thermodynamic model.[27] According to this model, the nucleation barrier for the formation of critical oxide embryo is given by

$$\Delta G^* = \frac{16\pi}{3g_v^2}\sigma_{NO}^3 h(\theta_1,\theta_2) \tag{1}$$

with

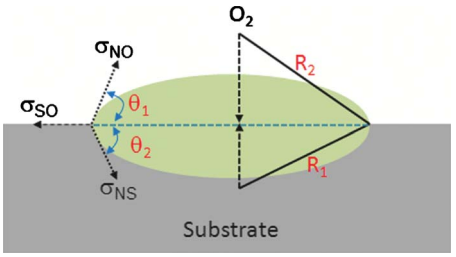

FIG. 2. (Color online) Heterogeneous nucleation of a double cap-shaped oxide island on a metal substrate, where the oxide nucleus embeds into the substrate due to the incorporation of underlying substrate atoms into the oxide phase. The upper cap has radius R_1 and contact angle θ_1, and the bottom cap has radius of R_2 and contact angle θ_2. σ_{NO}, σ_{NS}, and σ_{SO} represent the energies of the interfaces between the nucleus and oxygen gas, nucleus and substrate, and substrate and oxygen gas, respectively.

$$h(\theta_1,\theta_2)=\frac{\gamma}{\gamma-1}\left(\frac{\gamma-1}{\gamma}+\frac{\sin\theta_2}{\gamma\sin\theta_1}\frac{\sigma_{\mathrm{NS}}}{\sigma_{\mathrm{NO}}}\right)^3 f(\theta_1), \qquad (2)$$

where g_v is the free-energy change associated with oxidation of the metal. $h(\theta_1,\theta_2)$ is defined as the interfacial correlation function that governs the influence of surface reaction on the critical nucleation barrier in which $\gamma=V_{ox}/V_m$ is called the Pilling-Bedworth ratio,[28] where V_m and V_{ox} are the molar volume of the metal and the oxide, respectively; the interfacial contact angles θ_1 and θ_2 are related by the energy equilibrium condition $\sigma_{\mathrm{NO}}\cos\theta_1+\sigma_{\mathrm{NS}}\cos\theta_2-\sigma_{\mathrm{SO}}=0$ and $f(\theta)=\frac{(2+\cos\theta)(1-\cos\theta)^2}{4}$ is the geometrical factor for a plane surface.[29–32]

The kinetics of oxide nucleation is virtually characterized by the nucleation rate, which is defined as the number of stable nuclei created per area time. Oxygen molecules arriving from the vapor phase dissociate and migrate on the metal surface and then react with substrate atoms to produce oxide clusters of different sizes thus giving rise to critical nuclei. The number of nuclei formed in a fixed interval of time is a random quantity and is subject to statistical laws. The average values, however, can be calculated by the kinetic theory of nucleation. In nucleation, only islands of a size greater than a critical value will be stable and to grow, islands of this size are called critical nuclei. In classic nucleation theory, the rate of forming critical nuclei is considered to result from a two-step process, (i) the formation of a near equilibrium concentration, N^*, of critical nuclei and (ii) the impingement rate of adatoms, ω^*, upon these critical nuclei, which causes them to grow. Thus the nucleation rate, J, can be expressed as

$$J=\omega^* N^* \Gamma, \qquad (3)$$

where N^* is density of critical nuclei, ω^* is flux of attachment of adatoms to a critical nucleus, and Γ is called the Zeldovich factor.

The impingement of atoms onto a growing nucleus may occur by surface diffusion of adatoms to the nucleus periphery. The flux of oxygen toward the critical nucleus along the substrate surface can be calculated by

$$\omega^*=l^* D_s s\,\nabla(F\tau)\cong l^* D_s s\frac{F\tau}{a_0}, \qquad (4)$$

where l^* is the periphery of the nucleus on the substrate surface, D_s the oxygen atom jump rate, s the oxygen sticking coefficient, F the oxygen adsorption flux, τ the oxygen residence time, and a_0 the distance of a diffusion jump. The periphery of the critical nucleus, assuming a semispherical shape as shown in Fig. 2, is $2\pi R_1^*\sin\theta_1$, where θ_1 is the contact angle, R_1^* is the radius of the critical nucleus and can be calculated by $R_1^*=-\frac{2}{\gamma g_v}[(\gamma-1)\sigma_{\mathrm{NO}}+\frac{\sin\theta_2}{\sin\theta_1}\times\sigma_{\mathrm{NS}}]$.[27] D_s can be calculated by $D_s=a_0^2\upsilon_{\parallel}\exp(-\frac{E_{sd}}{kT})$, where a_0 is the distance of a diffusion jump, $\upsilon_{\parallel}$ the vibration frequency of oxygen atoms in a direction parallel to the surface plane; E_{sd} the activation energy for O surface diffusion, k the Boltzmann's constant, and T the oxidation temperature. The oxygen adsorption flux F can be calculated from the kinetic gas theory and is equal to $\frac{p_{\mathrm{O}_2}}{\sqrt{2\pi mkT}}$, where p_{O_2} is the oxygen gas pressure and m is the mass of an oxygen molecule. The residence time τ is equal to $\frac{1}{\upsilon_\perp}\exp(\frac{E_{des}}{kT})$, where $\upsilon_\perp$ is the atom vibration frequency of oxygen atoms in the direction normal to the surface plane and E_{des} denotes the activation energy for desorption. Assuming $\upsilon_\perp\approx\upsilon_\parallel\approx\upsilon$ for the frequency of attachment of oxygen atoms to the oxide nucleus,[33] one obtains

$$\omega^*=a_0 s 2\pi R_1^*\sin\theta_1\frac{p_{\mathrm{O}_2}}{\sqrt{2\pi mkT}}\exp\left(\frac{E_{des}-E_{sd}}{kT}\right). \qquad (5)$$

The equilibrium density N^* of critical nuclei depends on the nucleation barrier and the density of surface sites available for nucleation. It can be calculated by

$$N^*=N_s\exp\left(\frac{-\Delta G^*}{kT}\right), \qquad (6)$$

where ΔG^* is the free energy of formation of a critical oxide embryo and is given in Eq. (1), N_s is the concentration of O atoms at the surface and is the product of the adsorption flux F and the mean residence time τ,

$$N_s=\frac{p_{\mathrm{O}_2}}{\sqrt{2\pi mkT}}\frac{1}{\upsilon_\perp}\exp\left(\frac{E_{des}}{kT}\right). \qquad (7)$$

Because adsorbed oxygen atoms are localized at the metal surface, N_s must be replaced by the number of available adsorption sites in order to account for the configurational entropy that arises from the number of ways of arranging islands on the sites, i.e., there is a statistical contribution ΔG_{conf} to the work of the formation of oxide nuclei, which is independent of the nucleus size and accounts for the nucleus distribution and the single oxygen atoms among the available adsorption sites of density. Assuming the density of oxide islands is negligible compared with the concentration of adsorbed oxygen atoms, this energy contribution is

$$\Delta G_{conf}\approx -kT\ln\left(\frac{N_0}{N_s}\right), \qquad (8)$$

where N_0 is the density of available adsorption sites. As a result, the O concentration N_s is replaced by the density of the adsorption sites N_0.

According to the steady rate of nucleation, the Zeldovich factor Γ describes the deviation of the system from the equilibrium state and is directly proportional to the square of the supersaturation for the nucleation process. The steady-state distribution of islands may deviate perceptibly from the equilibrium one, N^*, in the vicinity of the critical size of the islands. Therefore, the Zeldovich factor is to correct for the fact that some islands that have reached the critical size still decay to smaller sizes. For a cap-shaped nucleus, Γ can be calculated by[33]

$$\Gamma=\frac{g_v^2}{8\pi\Omega\sqrt{kT\sigma_{\mathrm{NO}}^3 f(\theta_1)}}, \qquad (9)$$

where g_v is the free-energy change for the oxidation, Ω is the volume of oxygen atoms in the oxide phase, and $f(\theta_1)$ is the geometrical factor. For the oxidation of a metal $M+\frac{1}{2}\mathrm{O}_2$

$=MO$, the free-energy change per growth unit, g_v, can be written as

$$g_v = -\frac{1}{2N_A} RT \ln\left(\frac{p_{O_2}}{P^e_{O_2}}\right), \tag{10}$$

where N_A is the Avogadro constant, R the gas constant, T the oxidation temperature, p_{O_2} the actual oxygen pressure during the oxidation, and $p^e_{O_2}$ the equilibrium oxygen pressure as given by the Ellingham diagram for most metal oxides.[34] The value of $p^e_{O_2}$ for the oxidation of Cu into Cu_2O ($Cu+\frac{1}{2}O_2 = Cu_2O$) can be found in Fig. 5 (the black-dashed line).[34,35] $\frac{p_{O_2}}{P^e_{O_2}}$ can be considered as the supersaturation (i.e., the driving force) in the oxygen pressure for the oxidation. By substituting ω^*, N^*, and Γ using the expressions of Eqs. (5)–(10) into Eq. (3), the nucleation rate J can be obtained as

$$J/B = h'(\theta_1,\theta_2) P^e_{O_2}\left(\frac{p_{O_2}}{P^e_{O_2}}\right)\ln\left(\frac{p_{O_2}}{P^e_{O_2}}\right) \times \exp\left(-\frac{64\pi\Omega^2\sigma^3_{NO} h(\theta_1,\theta_2)}{3(kT)^3\left[\ln\left(\frac{p_{O_2}}{P^e_{O_2}}\right)\right]^2}\right) \tag{11}$$

with

$$B = \frac{a_0 s N_0}{4\gamma\sqrt{2\pi m\sigma_{NO}}}\exp\left(\frac{E_{des}-E_{sd}}{kT}\right) \tag{12}$$

and

$$h'(\theta_1,\theta_2) = \left[(\gamma-1)\sin\theta_1 + \frac{\sigma_{NS}}{\sigma_{NO}}\sin\theta_2\right][f(\theta_1)]^{-1/2}, \tag{13}$$

where $h'(\theta_1,\theta_2)$, like $h(\theta_1,\theta_2)$, is also a function of the "contact angles" θ_1 and θ_2.

III. DISCUSSION

We have shown in the previous section that the nucleation rate J is controlled by the supersaturation, i.e., the ratio of $\frac{p_{O_2}}{P^e_{O_2}}$, where $p^e_{O_2}$ can be obtained from bulk thermodynamics of the metal-oxide phase equilibria. To compare with experimental results, we will examine the nucleation kinetics as a function of the supersaturation at different oxidation temperatures. The phenomenon of kinetic hindrance in the initial oxide formation process has hitherto barely addressed, and quantitative experimental data on the nucleation kinetics is even fewer. Cu is one of the few metal systems which have been studied experimentally and quantitative nucleation data can be available in the literature. Therefore, our comparison between the theoretical model and experiments will be made for the oxidation of Cu, i.e., $2Cu+\frac{1}{2}O_2=Cu_2O$.

In Fig. 3, the nucleation rate J is plotted as a function of the supersaturation for an oxidation temperature $T=350$ °C with typical values of the quantities involved, i.e., Ω

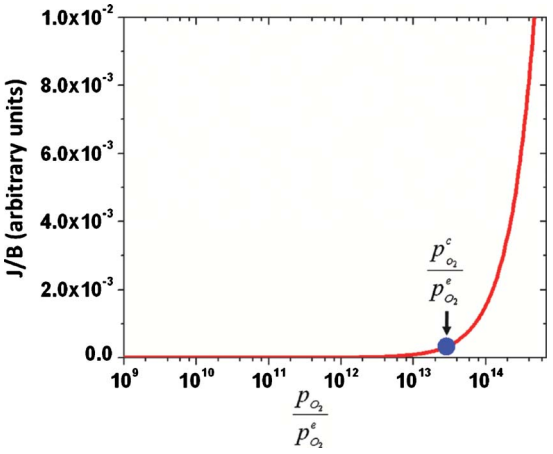

FIG. 3. (Color online) Dependence of the relative steady-state nucleation rate, J/B, on the supersaturation (here expressed in terms of the ratio of the oxygen pressures, i.e., $\frac{p_{O_2}}{P^e_{O_2}}$) for the oxidation at 350 °C. The critical supersaturation $\frac{p^c_{O_2}}{P^e_{O_2}}$ for the onset of an appreciable nucleation rate of oxide islands is marked by the arrow. As shown, many orders of magnitude higher in oxygen pressure than the equilibrium $p^e_{O_2}$ is required for the oxide nucleation.

$=a^2_{Cu_2O}/2$ for Cu_2O unit cell, $\gamma=a^3_{Cu_2O}/a^3_{Cu}\approx 1.6$, where $a_{Cu_2O}=4.22$ Å and $a_{Cu}=3.61$ Å are the lattice constants of Cu_2O and Cu, respectively; $\theta_2=1°$, and the surface energies of Cu [$\sigma_{SO}=1.3$ J/m^2 (Refs. 36 and 37)] and Cu_2O [$\sigma_{NO}=0.8$ J/m^2 (Ref. 38)]. The interface energy between Cu and Cu_2O is not readily available in the literature and is estimated as $\sigma_{NS}=(\sigma_{NO}+\sigma_{SO})/2$ by assuming an incoherent interface due to their large lattice misfit. As evident in Fig. 3, the nucleation rate is practically equal to zero and increases substantially only when the supersaturation $\frac{p^c_{O_2}}{P^e_{O_2}}$ is greater than some critical value, where $p^c_{O_2}$ denotes the critical oxygen pressure required for appreciable rate of oxide nucleation. The existence of such a critical supersaturation leads to the conclusion that nucleation of oxide islands will be experimentally observed only when $p_{O_2} > p^c_{O_2}$. In the opposite case, the oxygen gas and the metal will be in a metastable state, i.e., due to kinetic reasons no oxide nucleation will take place for the time of the experiment.

The onset of nucleation and growth processes can be identified from an experimental point of view by the observation of a sufficiently large number of newly formed oxide nuclei on the metal surface. Therefore, the experimentally determined critical supsaturation $\frac{p^c_{O_2}}{P^e_{O_2}}$ is related to the detection limit of the instrument employed in measuring the nucleation rate. Synchrotron x-ray surface scattering is very sensitive to island formation on the surface over large surface area[39] and has therefore been employed to determine the phase boundary between the metal and oxide phase during the oxidation of metals.[1,2] Using synchrotron x-ray surface scattering, Eastman *et al.* have determined the Cu_2O/Cu phase boundary during oxidation of a Cu(100) surface and the critical $p^c_{O_2}$ for the oxidation at 350 °C is $\sim 8.5\times 10^{-6}$ Torr. Since $p^e_{O_2}$ for the bulk Cu/Cu_2O phase equilib-

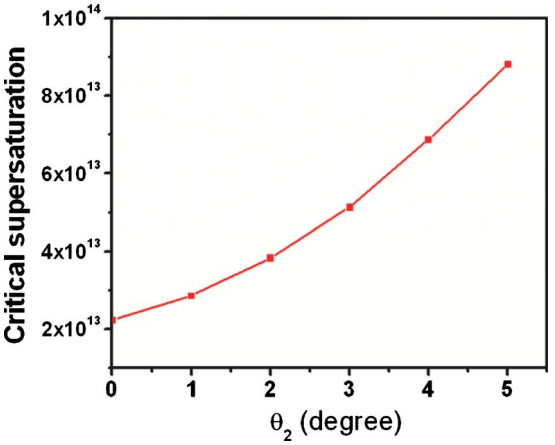

FIG. 4. (Color online) Dependence of the critical supersaturation, $\frac{p^c_{O_2}}{P^e_{O_2}}$, on the contact angle θ_2 of the oxide nucleus with the metal substrate for oxidation of Cu at 350 °C.

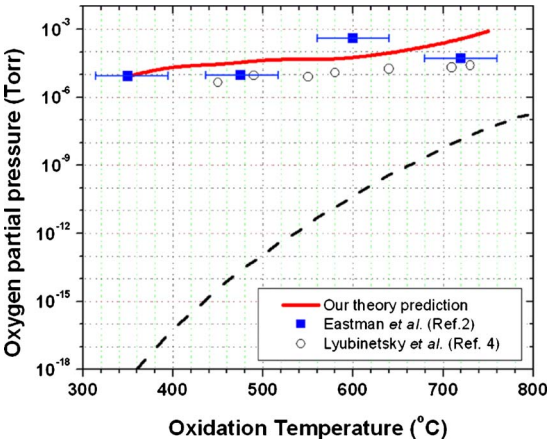

FIG. 5. (Color online) The red solid line shows the theoretical critical oxygen partial pressure $p^c_{O_2}$ for nucleation of Cu_2O islands on Cu(001) surfaces at different oxidation temperatures. Notably, this boundary of the oxygen partial pressure for oxide nucleation is several orders of magnitude larger than the bulk phase boundary (black-dashed line) (Refs. 34 and 35) and exhibits much less temperature dependence. The filled squares are the experimental data derived from Ref. 2 and the open circles are the experimental data derived from Ref. 4. Bulk phase diagram of the Cu_2O-Cu system is also shown (dashed lines).

rium at 350 °C is $\sim 3\times 10^{-19}$ Torr,[34,35] the critical supersaturation $\frac{p^c_{O_2}}{P^e_{O_2}}$ for the oxidation at this temperature is $\sim 2.8\times 10^{13}$, as marked in Fig. 3.

We then examine the effect of the interfacial functions $h(\theta_1,\theta_2)$ and $h'(\theta_1,\theta_2)$ on the critical supersaturation of oxygen pressure. The interfacial functions govern the influence of the gas-surface reaction on the oxide nucleation via the contact angle θ_2. The plot in Fig. 4 is obtained using Eq. (11) and depicts the dependence of the critical supersaturation $\frac{p^c_{O_2}}{P^e_{O_2}}$ on the contact angle θ_2 for the oxidation at 350 °C. It can be seen that $\frac{p^c_{O_2}}{P^e_{O_2}}$ increases with increasing the contact angle. $\theta_2=0$ corresponds to the situation where the oxide nuclei do not embed into the Cu substrate, which is possible if the oxide nucleation is via collisions of Cu and O atoms by surface diffusion, i.e., the formation of two-dimensional (2D) oxide nuclei. Although this 2D mechanism (i.e., $\theta_2=0$) requires a reduced $\frac{p^c_{O_2}}{P^e_{O_2}}$, the probability of forming oxide embryos via collisions of Cu and O atoms is small due to the large difference in the surface mobility of Cu and O atoms. This is because Cu atoms have to break neighboring bonds before they can move freely on the surface while impinging oxygen is highly mobile before they form chemical bonding with the substrate. Therefore, the oxide nucleation is dominated by the 3D nucleation mechanism where oxygen atoms diffuse over the substrate and react with underlying metal atoms. Thus, oxide nuclei embed into the substrate and $\theta_2>0$. This 3D nucleation mechanism is consistent with previous experimental results.[12,26,40–42] It can be noted in Fig. 4 that the variation in θ_2 from 0° to 5° causes no significant changes in the critical supersaturation (less than an order of magnitude). Due to their small sizes, oxide nuclei only slightly embed into the substrate, the use of a small contact angle ($\theta_2<5°$) would be a good approximation in the calculation.

Using the experimentally determined Cu_2O/Cu phase boundary $p^c_{O_2}\sim 8.5\times 10^{-6}$ Torr during the oxidation of Cu(100) at 350 °C as a reference for the detection limit in the synchrotron x-ray scattering experiments by Eastman *et al.*, we can then determine the critical oxygen pressures $p^c_{O_2}$ for the nucleation of Cu_2O islands at all other oxidation temperatures with use of the nucleation rate Eq. (11). Having thus established the means to determine the critical oxygen pressure $p^c_{O_2}$ for the nucleation of oxide islands, we can in a straightforward way construct a diagram showing the critical oxygen pressure $p^c_{O_2}$ with the limit of metastability of the ambient oxygen phase with the metal substrate over a wide range of oxidation temperature and oxygen pressure. The result is shown in Fig. 5, covering the range of the oxidation temperature from 350 to 800 °C. Our calculations of the critical oxygen pressure $p^c_{O_2}$ provide satisfactory agreement with the experimental data obtained from the wide range of the oxidation temperature.[2,4] For comparison purposes, Fig. 5 also displays the bulk Cu-Cu_2O phase diagram.[34,35] The limit of the metastability of oxygen gas with Cu as determined from our kinetic model reveals a striking difference in behavior compared to the bulk phase diagram, with the many orders of magnitude upward in oxygen pressure for oxide nucleation, particularly at lower temperatures, and exhibiting weak temperature dependence, which is also in good agreement with these reported experimental data, as shown in Fig. 5.

Two prominent features can be noted from Fig. 5: (i) the phase boundary (i.e., $p^c_{O_2}$) between oxygen gas and a clean Cu surface is much higher than the bulk Cu_2O/Cu phase equilibria ($p^e_{O_2}$). This significantly increased oxygen pressure for the initial oxide formation is due to the critical supersaturation required for the onset of an appreciable nucleation rate of oxide islands. (ii) The temperature dependence of the phase boundary between oxygen gas and the clean Cu surface is much weaker than that for the bulk Cu_2O/Cu phase equilibria. This weak temperature dependence can be under-

stood from Eq. (11), where $\frac{p^c_{O_2}}{p^e_{O_2}}$ plays a more dominant role in determining the overall nucleation rate J than the oxidation temperature T since the critical oxygen pressure $p^c_{O_2}$ is many orders of magnitude higher than $p^e_{O_2}$ (i.e., in the exponential term, the nucleation rate J is less sensitive to the oxidation temperature than the oxygen pressure under the required supersaturation in oxygen pressure).

IV. CONCLUSION

In summary, aiming at understanding the phenomenon of kinetic hindrance to the oxide formation during the initial stages of oxidation of metals, we proposed a kinetic model to describe the nucleation of oxide islands. Our results show that the nucleation of oxide islands requires a critical oxygen pressure, $p^c_{O_2}$, below which the nucleation rate is practically equal to zero and increases substantially beyond it. This critical oxygen partial pressure shows very little temperature dependence and is many orders of magnitude higher than the equilibrium partial pressure predicted from the bulk thermodynamics. The theoretical results provide good agreement with reported experimental data obtained over a large range of oxidation temperature. We expect that the insights obtained from this study have broader implications in understanding and manipulating transient oxidation of metals, where oxide islanding generally occurs but the information on the fundamental processes is still very limited. Such a kinetic hindrance in the initial oxidation could be also crucial for understanding high-pressure applications such as oxidation and reduction reactions under ambient working atmosphere in heterogeneous catalysis.

ACKNOWLEDGMENT

Research was supported by the U.S. Department of Energy, Office of Basic Energy Sciences, Division of Materials Sciences and Engineering under Grant No. DE-FG02-09ER46600.

*gzhou@binghamton.edu

[1] E. Lundgren, J. Gustafson, A. Mikkelsen, J. N. Andersen, A. Stierle, H. Dosch, M. Todorova, J. Rogal, K. Reuter, and M. Scheffler, Phys. Rev. Lett. **92**, 046101 (2004).
[2] J. A. Eastman, P. H. Fuss, L. E. Rehn, P. M. Baldo, G. W. Zhou, D. D. Fong, and L. J. Thompson, Appl. Phys. Lett. **87**, 051914 (2005).
[3] K. Lahtonen, M. Hirsimaki, M. Lampimaki, and M. Valden, J. Chem. Phys. **129**, 124703 (2008).
[4] I. Lyubinetsky, S. Thevuthasan, D. E. McCready, and D. R. Baer, J. Appl. Phys. **94**, 7926 (2003).
[5] C. I. Carlisle, T. Fujimoto, W. S. Sim, and D. A. King, Surf. Sci. **470**, 15 (2000).
[6] N. Al-Sarrafa, J. T. Stucklessa, C. E. Wartnaby, and D. A. King, Surf. Sci. **283**, 427 (1993).
[7] W. A. Brown, R. Kose, and D. A. King, Chem. Rev. **98**, 797 (1998).
[8] J. T. Stuckless, N. Al-Sarraf, C. E. Wartnaby, and D. A. King, J. Chem. Phys. **99**, 2202 (1993).
[9] J. T. Stuckless, C. E. Wartnaby, N. Al-Sarraf, S. J. Dixon-Warren, M. Kovar, and D. A. King, J. Chem. Phys. **106**, 2012 (1997).
[10] J. C. Yang, M. Yeadon, B. Kolasa, and J. M. Gibson, Scr. Mater. **38**, 1237 (1998).
[11] G. W. Zhou and J. C. Yang, Phys. Rev. Lett. **89**, 106101 (2002).
[12] G. W. Zhou and J. C. Yang, Surf. Sci. **531**, 359 (2003).
[13] G. W. Zhou and J. C. Yang, Appl. Surf. Sci. **210**, 165 (2003).
[14] G. W. Zhou and J. C. Yang, J. Mater. Res. **20**, 1684 (2005).
[15] S. Aggarwal, A. P. Monga, S. R. Perusse, R. Ramesh, V. Ballarotto, E. D. Williams, B. R. Chalamala, Y. Wei, and R. H. Reuss, Science **287**, 2235 (2000).
[16] H. Niehus and C. Achete, Surf. Sci. **369**, 9 (1996).
[17] P. H. Holloway and J. B. Hudson, Surf. Sci. **43**, 123 (1974).
[18] K. R. Lawless, Rep. Prog. Phys. **37**, 231 (1974).
[19] S. R. Shinde, A. S. Ogale, S. B. Ogale, S. Aggarwal, V. A. Novikov, E. D. Williams, and R. Ramesh, Phys. Rev. B **64**, 035408 (2001).
[20] G. W. Zhou, L. Wang, R. C. Birtcher, P. M. Baldo, J. E. Pearson, J. C. Yang, and J. A. Eastman, Phys. Rev. Lett. **96**, 226108 (2006).
[21] G. W. Zhou, J. A. Eastman, R. C. Birtcher, P. M. Baldo, J. E. Pearson, L. J. Thompson, L. Wang, and J. C. Yang, J. Appl. Phys. **101**, 033521 (2007).
[22] K. Heinemann, D. B. Rao, and D. L. Douglas, Oxid. Met. **11**, 321 (1977).
[23] J. C. Yang, Z. Q. Li, L. Sun, G. W. Zhou, J. A. Eastman, D. D. Fong, P. H. Fuoss, P. M. Baldo, L. E. Rehn, and L. J. Thompson, Mater. High. Temp. **26**, 1 (2009).
[24] E. E. Hajcsar, P. R. Underhill, and W. W. Smeltzer, Langmuir **11**, 4862 (1995).
[25] P. H. Holloway and J. B. Hudson, Surf. Sci. **43**, 141 (1974).
[26] J. C. Yang, M. Yeadon, B. Kolasa, and J. M. Gibson, Appl. Phys. Lett. **70**, 3522 (1997).
[27] G. W. Zhou, Appl. Phys. Lett. **94**, 201905 (2009).
[28] N. Birks, G. H. Meier, and F. S. Pettit, *Introduction to the High Temperature Oxidation of Metals* (Cambridge University Press, Cambridge, 2006).
[29] D. Turnbull and B. Vonnegut, Ind. Eng. Chem. **44**, 1292 (1952).
[30] X. Y. Liu, J. Chem. Phys. **112**, 9949 (2000).
[31] X. Y. Liu, Langmuir **16**, 7337 (2000).
[32] X. Y. Liu, J. Chem. Phys. **111**, 1628 (1999).
[33] I. V. Markov, *Crystal Growth for Beginners: Fundamentals of Nucleation, Crystal Growth, and Epitaxy* (World Scientific, New Jersey, 1995).
[34] D. R. Gaskell, *Introduction to Metallurgical Thermodynamics* (Scripta, Washington, DC, 1973).
[35] R. D. Schmidt-Whitley, M. Martinez-Clemente, and A. Revcolevschi, J. Cryst. Growth **23**, 113 (1974).
[36] S. M. Foiles, M. I. Baskes, and M. S. Daw, Phys. Rev. B **33**, 7983 (1986).

[37] Y. N. Wen and J. M. Zhang, Solid State Commun. **144**, 163 (2007).
[38] A. Soon, M. Todorova, B. Delley, and C. Stampfl, Phys. Rev. B **75**, 125420 (2007).
[39] P. H. Fuoss and S. Brennan, Annu. Rev. Mater. Sci. **20**, 365 (1990).
[40] G. W. Zhou and J. C. Yang, Appl. Surf. Sci. **222**, 357 (2004).
[41] G. W. Zhou and J. C. Yang, Phys. Rev. Lett. **93**, 226101 (2004).
[42] G. W. Zhou, W. Y. Dai, and J. C. Yang, Phys. Rev. B **77**, 245427 (2008).